

## PAPR and Spectral Control Procedure for OFDM Wireless Systems Using CAZAC Equalization

Yoshitsugu Sugai, Yushi Shirato, Tomotaka Kimura and Masahiro Muraguchi

Department of Electrical Engineering, Tokyo University of Science  
6-3-1 Nijjuku, Katsushika-ku, Tokyo, Japan

E-mail: 4317614@ed.tus.ac.jp, yshirato@sea.plala.or.jp, kimura, murag@ee.kagu.tus.ac.jp

**Abstract**— A major drawback of Orthogonal Frequency Division Multiplexing (OFDM) signals is extremely high Peak-to-Average Power Ratio (PAPR). The CAZAC equalization scheme makes the PAPR of M-array Quadrature Amplitude Modulation (M-QAM) OFDM signals into the PAPR of M-QAM single-carrier signals. Therefore, it dramatically improves the PAPR of OFDM signals. However, severe bandpass filtering of CAZAC-OFDM signal lead to unacceptable degradation of the PAPR. The paper provides available control procedure for PAPR and spectrum managements. It is confirmed that the CAZAC-OFDM signal controlled by our procedure maintains enough low PAPR and can clear the spectrum mask specifications in IEEE802.11 standard.

**Keywords**-OFDM; CAZAC; spectrum mask; PAPR.

### I. INTRODUCTION

Orthogonal Frequency Division Multiplex (OFDM) systems that attain high speeds and high capacity have recently been attracting attention in wireless applications, e.g., Wireless Local Area Networks (WLANs), third Generation Partnership Project Long-Term Evolution (3GPP LTE), and the Digital Video Broadcasting-Terrestrial (DVB-T) standard [1][2]. However, the main drawback of OFDM is its high Peak-to-Average Power Ratio (PAPR), which decreases the efficiency of Power Amplifiers (PAs) and increases transmitter power consumption [3][4]. Therefore, a number of techniques have been proposed to reduce the PAPR [3]. Well-known techniques are clipping-and-filtering, Partial Transmit Sequences (PTSSs), and Selected Mapping (SLM). Clipping-and-filtering limits the peak amplitude of the transmission signal. However, non-linear distortion causes BER to degrade. PTS partitions input data into disjoint sub-blocks. Moreover, each sub-block are weighted by a phase factor. This technique chooses the phase factor to minimize the PAPR of combined signals. SLM generates multiple candidate data blocks. All data blocks represent the same information. Although PTS and SLM can be expected to create a certain reduction in PAPR, both techniques need side information in the receiver, which decreases spectral efficiency. The most practical solution to improving PAPR is to introduce Single Carrier Frequency Division Multiplexing Access (SC-FDMA). The 3GPP LTE system adopts SC-FDMA for uplink multiple access systems [2][5]. However, SC-FDMA has not been considered to be suitable for next-

generation high-speed communications.

A new PAPR reduction technique with Constant Amplitude Zero Auto-Correlation (CAZAC) equalization was recently proposed [6][7]. The CAZAC equalization scheme makes the PAPR of M-array Quadrature Amplitude Modulation (M-QAM) OFDM signals into the PAPR of M-QAM single-carrier signals [8]. Therefore, it dramatically improves the PAPR of OFDM signals. However, severe bandpass filtering of CAZAC-OFDM signal lead to unacceptable degradation of the PAPR.

The paper provides available control procedure for PAPR and spectrum managements for the CAZAC-OFDM system. One simplest approach of improving the PAPR is to clip the amplitude of the signal to a fixed level. An accurate clipping boundary is easily defined, because we can manage the amplitude of the time-domain signal of CAZAC-OFDM like a single-carrier signal. As the correct demodulation of CAZAC-OFDM signals requires only values of the original signal points, we can improve the PAPR without any degradation of BER and spectrum performances by clipping. We have confirmed that the CAZAC-OFDM signal controlled by our procedure maintains enough low PAPR and can clear the spectrum mask specifications in IEEE802.11 standard.

The rest of this paper is organized as follows. In Section 2, we describe the CAZAC-OFDM system. In Section 3, we describe the proposed spectral control. In Section 4, we describe the PAPR reduction method. Finally, we conclude this paper in Section 5.

### II. CAZAC-OFDM SYSTEM

In this section, we describe the CAZAC-OFDM System. We first describe the OFDM system, and then we explain the CAZAC equalizing technique.

#### A. OFDM system

In OFDM system, the frequency domain symbol  $\mathbf{X} = [X_0, X_1, \dots, X_{N-1}]^T$  is modulated by  $N$  size inverse Fast Fourier Transform (IFFT). The discrete-time OFDM signal with  $N$  subcarriers is represented as

$$x_n = \sum_{k=0}^{N-1} X_k e^{j2\pi kn/N}, \quad (1)$$

where  $j = \sqrt{-1}$  and  $n$  is discrete time index. On the other hand, receiver acquires frequency domain symbol  $\mathbf{Y}$  by applying FFT to received signal  $\mathbf{y}$ .

$$Y_k = \sum_{n=0}^{N-1} y_n e^{-j2\pi kn/N} = \sum_{n=0}^{N-1} (x_n + \text{Noise}) e^{-j2\pi kn/N}. \quad (2)$$

The PAPR of the OFDM signal (1) can be expressed as

$$PAPR = \frac{\max_{0 \leq n \leq N-1} |x_n|^2}{E[|x_n|^2]}, \quad (3)$$

where  $E[\cdot]$  is expectation operator. PAPR represents amplitude fluctuation of each symbol. In order to improve the accuracy of PAPR, the OFDM signal  $x_k$  is converted to  $L$ -times oversampled time domain signal [1].

As shown from (2), the OFDM signal is composed of a plurality of subcarrier signals, which causes an increase in amplitude fluctuation. A high PAPR signal increases the Input Back Off (IBO) at the power amplifier in order to amplify the transmit signal without distortion. In general, increasing in IBO causes decreasing the efficiency of PA.

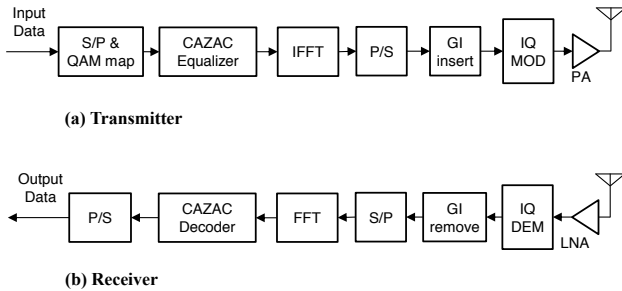


Figure 1. CAZAC-OFDM system.

### B. CAZAC equalizing technique

Figure 1 shows a transmitter and receiver block diagrams for a CAZAC-OFDM system. The CAZAC sequence is an orthogonal sequence and the autocorrelation function is a delta function. In addition, the CAZAC sequence has a characteristic that the amplitude exhibits a constant value in both time and frequency domain. Zadoff-Chu (ZC) sequences is one of the CAZAC sequence. The ZC sequence  $C_k$  of length  $L$  is defined as

$$C_k = \begin{cases} \exp\left(\frac{j\pi k(k-1)r}{L}\right) & (L \text{ is odd}) \\ \exp\left(\frac{j\pi(k-1)^2 r}{L}\right) & (L \text{ is even}) \end{cases}, \quad (4)$$

where  $L$  is the length of the CAZAC sequence and  $r$  is the sequence number,  $k = 1, 2, \dots, L$ .  $L$  is a natural number, and  $r$  is a prime integer with respect to  $L$ . CAZAC sequences are generated by cyclic shift of the original CAZAC sequence. The periodic cross-correlation function  $\rho$  is defined as

$$\rho(m) = \sum_{n=1}^{L-1} c_n c_{(c-m) \bmod L}^* = \begin{cases} L & (m = 0) \\ 0 & (m \neq 0) \end{cases}, \quad (5)$$

where  $m$  is integer variables.

CAZAC equalization uses a square matrix  $M$  generated from the equation in the case where  $L$  in equation (4) is an even number. The matrix equation is defined as

$$M = \frac{1}{\sqrt{N}} \begin{bmatrix} c_1 & c_2 & \dots & c_N \\ c_{N+1} & c_{N+2} & \dots & c_{2N} \\ \vdots & \vdots & \ddots & \vdots \\ c_{(N-1)N+1} & \dots & \dots & c_{N^2} \end{bmatrix}, \quad (6)$$

where matrix  $M$  is the rearrangement of in equation (4) in the row direction, and  $N$  is the number of subcarriers and  $L = N^2$ ,  $r = 1$ .  $N$  is an even number, so  $L$  is also an even number.

Multiply the signal before IFFT by the matrix as shown in Figure 1 calculate the product of the transposed the frequency domain symbol  $X = [X_1, X_2, \dots, X_N]$  and the matrix  $M$ , and create a CAZAC equalized signal  $X'$ .  $X'$  is represented as

$$X' = M \cdot X^T = \frac{1}{\sqrt{N}} \begin{bmatrix} c_1 & \dots & c_N \\ c_{N+1} & \dots & c_{2N} \\ \vdots & \ddots & \vdots \\ c_{(N-1)N+1} & \dots & c_{N^2} \end{bmatrix} \cdot \begin{bmatrix} X_1 \\ X_2 \\ \vdots \\ X_N \end{bmatrix}. \quad (7)$$

An IFFT operation is performed on this signal. The OFDM time domain signal  $x_n$  of the sample is represented as

$$x_n = \frac{1}{N} \sum_{k=0}^{N-1} X'_k e^{j2\pi kn/N} = \sum_{k=0}^{N-1} \left\{ \sum_{m=0}^{N-1} e^{j\pi(m+kN)^2/L} X_m \right\} e^{j2\pi kn/N} = \sum_{m=0}^{N-1} e^{j\pi m^2/N^2} X_m \left\{ \sum_{k=0}^{N-1} e^{j2\pi k(m+n)/N} e^{j\pi k^2} \right\}, \quad (8)$$

where  $k$  is an integer not less than 0, so the following equation is developed.

$$\exp(j\pi k^2) = \begin{cases} 1 & (k : \text{even}) \\ -1 & (k : \text{odd}) \end{cases}. \quad (9)$$

To lead (10) from (9).

$$\exp(j\pi k^2) = (-1)^k. \quad (10)$$

Substituting (10) into (8) leads to (11).

$$x_n = \sum_{m=0}^{N-1} e^{j\pi m^2/N^2} X_m \left\{ \sum_{k=0}^{N-1} \{-e^{j2\pi(m+n)/N}\}^k \right\}. \quad (11)$$

The inside of  $\{\}$  in equation (11) is the sum of the geometric progression. Therefore, equation (12) is derived.

$$\begin{aligned} \sum_{k=0}^{N-1} \{-e^{j2\pi(m+n)/N}\}^k \\ = \begin{cases} N & (-e^{j2\pi(m+n)/N} = 1) \\ 0 & (-e^{j2\pi(m+n)/N} \neq 1) \end{cases}. \end{aligned} \quad (12)$$

When  $2\pi(m+n)/N = 1$ ,  $2(m+n)/N$  is an integer and odd number. Also,  $n$  and  $m$  are  $0 \leq n \leq N-1, 0 \leq m \leq N-1$ . These relationships satisfy the relationship of equation (13).

$$m = \frac{N}{2} - n \pmod{N}. \quad (13)$$

Equation (14) is derived from equations (11), (12) and (13).

$$\begin{aligned} x_n &= e^{j\pi\{N/2-n \pmod{N}\}^2/N^2} X_{\frac{N}{2}-n \pmod{N}} \\ &= c_{\frac{N}{2}-n \pmod{N}} X_{\frac{N}{2}-n \pmod{N}}, \end{aligned} \quad (14)$$

Equation (14) shows that CAZAC equalization converts the PAPR of the OFDM time domain signal into the PAPR of a single-carrier signal. Figure 2 shows the image diagram of the CAZAC-OFDM time domain signal. Among the components of the coefficient  $X$ , only one was reinforced, all others cancel each other.

Figures 3 (a) and (b) show the constellation of CAZAC-OFDM, which shows time-domain signal points at the IQ-MOD input in Figure 1. The discrete-time signal points of QPSK CAZAC-OFDM line up on the unit circle orbit as shown in Figure 3 (a), and the discrete-time signal points of 16QAM CAZAC-OFDM signal are on the three concentric circle orbits as shown in Figure 3 (b).

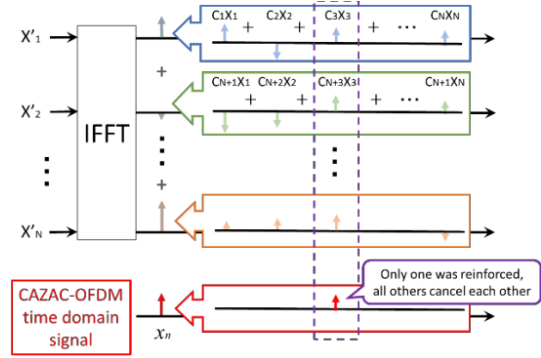


Figure 2. The time domain signal of CAZAC-OFDM

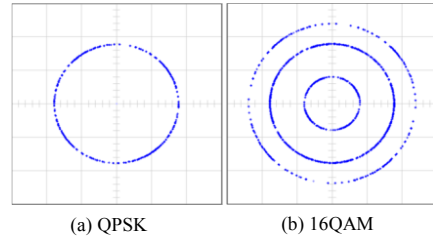


Figure 3. Constellation examples of the CAZAC-OFDM Signals.

### III. SPECTRAL CONTROL

In this section, we explain the proposed spectral control method. We first describe the procedure of the proposed method, and then we evaluate the performance of the spectral control method through simulation experiments.

#### A. Procedure of Spectral Control

The CAZAC-OFDM signal at the IQ-MOD output in Figure 1 is an analog signal wave, which deals with the passband signal with a carrier frequency of  $f_c$  in the continuous time domain. Since  $f_c$  in general is much higher than  $1/T_s$ , a continuous-time baseband OFDM signal with the symbol period  $T_s$  and the corresponding passband signal with the carrier frequency  $f_c$  have almost the same waveform. However, in general, the waveform for the discrete-time baseband signal may not be the same as that for the continuous-time baseband signal. In practice, the PAPR for the continuous-time baseband signal can be measured only after implementing the actual hardware, including Digital-to-Analog Converter (DAC). In other words, measurement of the PAPR for the continuous-time baseband signal is not straightforward. Therefore, there must be some means of estimating the PAPR from the discrete-time signal. Fortunately, it is known that the discrete-time baseband signal can show almost the same PAPR as the continuous-time baseband signal if it is four times interpolated (oversampled).

To make the discrete-time OFDM signal with the proper passband characteristics which satisfy the IEEE 802.11 specifications, we set the subcarrier allocation as shown in Figure 4. Here, we set the FFT size of CAZAC-OFDM to 64. Therefore, four times interpolated (oversampled) FFT size

becomes 256.

The first task to consider is that the CAZAC-OFDM spectrum of 64 subcarriers with the bandwidth (BW) of 16MHz is centered on the carrier frequency of  $f_c$ , 24MHz bandwidth to the left, i.e., the space of 96 null subcarriers, and in the same way 24 MHz bandwidth to the right. Figure 5 shows a block diagram of the generation of CAZAC-OFDM symbols. The second step to produce the signal is to apply a transmit filtering with proper roll-off by an FFT-window processing, and to avoid aliasing by low-pass filtering. Figure 6 shows a block diagram of the reproduction of CAZAC-OFDM symbols. In receiver side, multiply the received symbol in frequency domain and the inverse matrix  $(M^T)^H$  after FFT shown by figure 6.

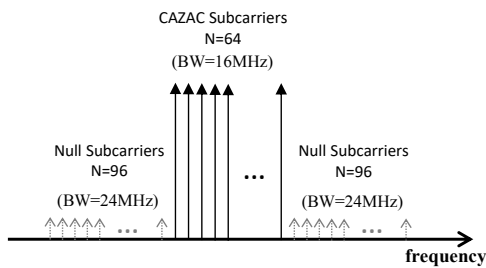


Figure 4. Subcarrier allocation based on four times interpolated (oversampled) FFT processing.

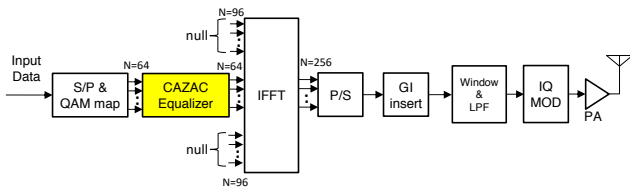


Figure 5. The CAZAC-OFDM transmitter based on four times interpolated (oversampled) FFT processing.

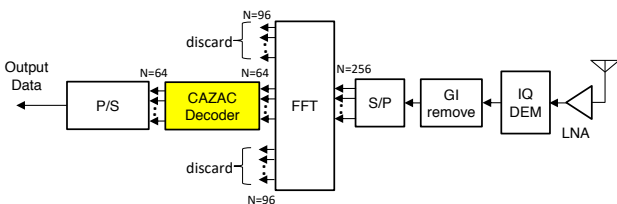


Figure 6. The receiver block diagram for spectral controlled CAZAC-OFDM signal.

**B. Simulation results**

We carried out our simulation with the MATLAB/ Simulink to evaluate the performance of the system. Table I summarizes the simulation parameters.

Figure 7 shows the spectrum for the 16QAM CAZAC-OFDM system. It is confirmed that the spectrum satisfied the spectrum mask standardized by the IEEE 802.11 specifications [1].

TABLE I. MAJOR SIMULATION PARAMETERS

Number of CAZAC Subcarriers	64 [Data: 60, Pilot: 4]
IFFT & FFT size	256
Sampling Rate	16MHz
Symbol Period $T_s$	5 $\mu$ sec
Guard Interval	1 $\mu$ sec
Modulation of Subcarriers	QPSK, 16QAM
Channel Model	AWGN
	Flat Rayleigh Fading - Doppler Frequency( $f_b T_s$ ): $7.5 \times 10^{-5}$
	18-Ray Rayleigh Fading with Exponential Decay Profile - Doppler Frequency( $f_b T_s$ ): $7.5 \times 10^{-5}$ - Delay Spread( $\tau/T_s$ ): $2 \times 10^{-2}$

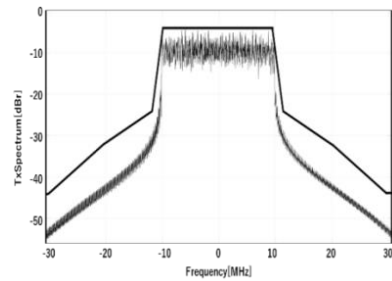


Figure 7. The spectrum controlled 16QAM CAZAC-OFDM signal.

**IV. PAPR CONTROL**

This section describes the proposed PAPR control method. We first explain the procedure of the PAPR control method, and then we present simulation results to discuss the performance of the proposed PAPR control method.

**A. Procedure of PAPR control**

The CAZAC equalization scheme makes the PAPR of M-array Quadrature Amplitude Modulation (M-QAM) OFDM signals into the PAPR of M-QAM single-carrier signals. Therefore, it dramatically improves the PAPR of OFDM signals. However, severe bandpass filtering of the CAZAC-OFDM signal lead to unacceptable degradation of the PAPR.

Figure 8 shows the amplitude of bandpass and four times oversampled QPSK CAZAC-OFDM signal with subcarrier allocation shown in Figure 4. The original sample points of QPSK are on the line of unity amplitude. However, many of the interpolating points go above the line of unity amplitude. This means obvious degradation of the PAPR.

One simplest approach of reducing the PAPR is to clip the amplitude of the signal to a fixed level. Fortunately, correct demodulation of CAZAC-OFDM signals requires only values of the original sample points, and it is possible to skip out the values of the interpolating points. Therefore, we can clip amplitude of the interpolating points at the unity

amplitude level as the clipping boundary in case of the QPSK CAZAC-OFDM signal.

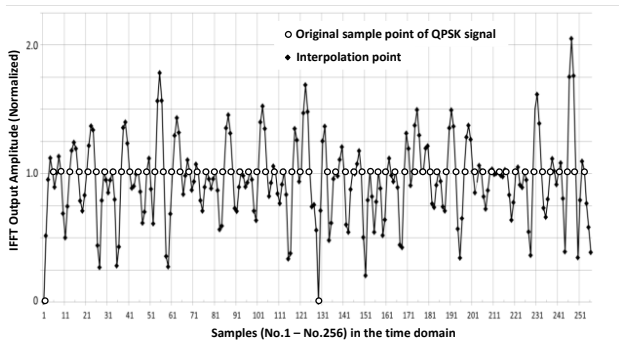


Figure 8. Amplitude of bandpass and oversampled QPSK CAZAC-OFDM signal in the time domain.

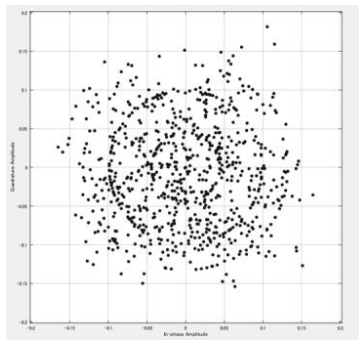


Figure 9. The constellation of bandpass and oversampled 16-QAM CAZAC-OFDM signal.

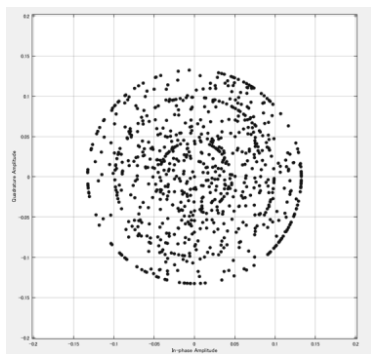


Figure 10. The constellation of bandpass and oversampled 16-QAM CAZAC-OFDM signal with clipped amplitude processing.

**B. Simulation results**

Figure 9 shows the constellation of bandpass and four times oversampled 16QAM CAZAC-OFDM signal with subcarrier allocation shown in Figure 4. The original sample points of 16QAM CAZAC-OFDM signal are on the three concentric circle orbits as shown in Figure 3 (b). However, many of the interpolating points overfly to outer side of the largest circle orbit. This means obvious degradation of the

PAPR.

As noted previously, correct demodulation of CAZAC-OFDM signals requires only values of the original sample points, which are all in the inner-side of the largest circle orbit of 16QAM CAZAC-OFDM signal, and it is possible to clip amplitude of the interpolating sample points. Figure 10 shows the constellation of bandpass and oversampled 16-QAM CAZAC-OFDM signal with clipped amplitude processing.

We first considered the Complementary Cumulative Distribution Function (CCDF) of PAPR to evaluate the performance of PAPR, which is the probability that PAPR will be higher than a certain PAPR value  $PAPR_0$ , i.e.,  $Pr(PAPR > PAPR_0)$ . Figure 11 plots the CCDF of PAPR of 16QAM CAZAC-OFDM system with and without clipping, as well as the conventional 16QAM OFDM and single-carrier 16QAM systems. We found that the PAPR of the 16QAM CAZAC-OFDM system with clipping was almost equal to that of the single-carrier 16QAM system. Moreover, the PAPR of the 16QAM CAZAC-OFDM system with clipping was improved by 5 dB at the CCDF of  $10^{-3}$  compared with the conventional 16QAM OFDM system.

Figure 12 shows spectrum for the 16QAM CAZAC-OFDM system with clipping. It is confirmed that the spectrum also satisfied the spectrum mask standardized by the IEEE 802.11 specifications. The result indicates the clipping does not bring serious effect to the spectrum.

We next examined the Bit Error Rate (BER) of the proposed system. We considered three channels: Additive White Gaussian Noise (AWGN) and two type of Rayleigh fading with AWGN.

Figure 13 shows the BER performances of the QPSK and the 16QAM CAZAC-OFDM systems with clipping which are applied for AWGN channels. The results indicate that the CAZAC-OFDM system with clipping does not degrade BER performances.

Figure 14 shows the BER performances of the 16QAM CAZAC-OFDM system with clipping which are applied for fading channels. We found that the BER of the system was comparable to that of the conventional OFDM system under the Flat Rayleigh Fading channel. In contrast, under the 18-Ray Rayleigh Fading channel, which is a type of frequency selective fading channel, the BER of the 16QAM CAZAC-OFDM system with clipping is improved because the influence of fading is spread to all sub-carriers. This indicates that the CAZAC-OFDM system has excellent capabilities to resist frequency selective fading.

**V. CONCLUSIONS**

The paper provides available control procedure for PAPR and spectrum managements for the CAZAC-OFDM system. One simplest approach of improving the PAPR is to clip the amplitude of the signal to a fixed level. An accurate clipping boundary is easily defined, because we can manage the amplitude of the time-domain signal of CAZAC-OFDM like a single-carrier signal. As the correct demodulation of

CAZAC-OFDM signals requires only values of the original signal points, we can improve the PAPR without any degradation of BER and spectrum performances by clipping. We have confirmed that the 16QAM CAZAC-OFDM signal controlled by our procedure maintains enough low PAPR of 6dB and can clear the spectrum mask specifications in IEEE802.11 standard. Moreover, under the 18-Ray Rayleigh Fading channel, which is a type of frequency selective fading channel, the BER of the 16QAM CAZAC-OFDM system with clipping is improved, compared with the conventional OFDM system, because the influence of fading is spread to all sub-carriers. This indicates that the CAZAC-OFDM system has excellent capabilities to resist frequency selective fading.

REFERENCES

- [1] IEEE, "Part 11: Wireless LAN Medium Access Control (MAC) and Physical Layer (PHY) Specifications," IEEE Std 802.11-2012 (Revision of IEEE Std 802.11-2007), Mar. 2012, pp. 1-2695.
- [2] A. Ghosh, R. Ratasuk, B. Mondal, N. Mangalvedhe, and T. Thomas, "LTE-advanced: Next-generation Wireless Broadband Technology," IEEE Wireless Communications, vol. 17, no. 3, June 2010, pp. 10–22.
- [3] H. Seung, Hee and L. Jae, Hong, "An Overview of Peak-to-average Power Ratio Reduction Techniques for Multicarrier Transmission," IEEE Wireless Communications, vol. 12, no. 2, Apr. 2005, pp. 56–65.
- [4] J. Joung, C. K. Ho, K. Adachi, and S. Sun, "A Survey on Power-Amplifier-Centric Techniques for Spectrum- and Energy-Efficient Wireless Communications," IEEE Communications Surveys & Tutorials, vol. 17, no. 1, Jan. 2015, pp. 315–333.
- [5] H. Myung, J. Lim, and D. Goodman, "Single Carrier FDMA for Uplink Wireless Transmission," IEEE Vehicular Technology Magazine, vol. 1, no. 3, Sep. 2006, pp. 30-38.
- [6] I. Baig and V. Jeoti, "PAPR Reduction in OFDM Systems: Zadoff-Chu Matrix Transform Based Pre/Post-Coding Techniques," in Proc. of the 2nd International Conference on Computational Intelligence, Communication Systems and Networks, July 2010, pp. 373-377.
- [7] Z. Feng, et al., "Performance-Enhanced Direct Detection Optical OFDM Transmission With CAZAC Equalization," IEEE Photonics Technology Letters, vol. 27, no. 14, July 2015, pp. 1507-1510.
- [8] R. Ishioka, T. Kimura, and M. Muraguchi, "A Proposal for a New OFDM Wireless System using a CAZAC Equalization Scheme," Proc. AICT 2017, June 2017, pp. 47-51.

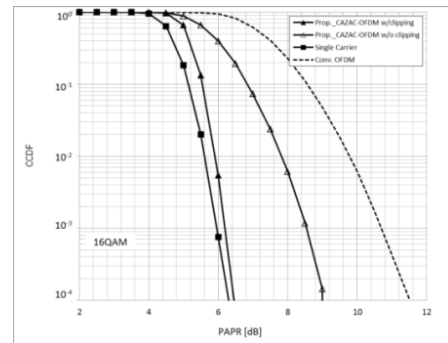


Figure 11. PAPR of the proposed CAZAC-OFDM.

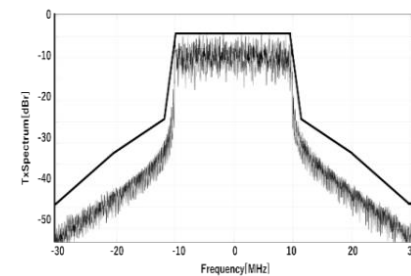


Figure 12. Spectrum of the 16QAM CAZAC-OFDM Signal with clipping.

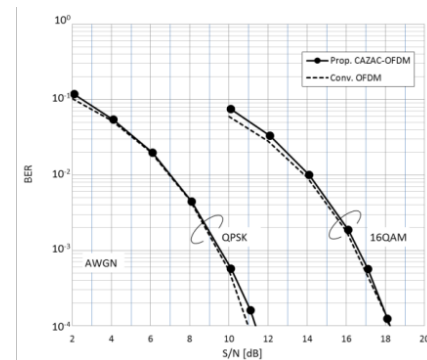


Figure 13. BER performances of the systems under AWGN channels.

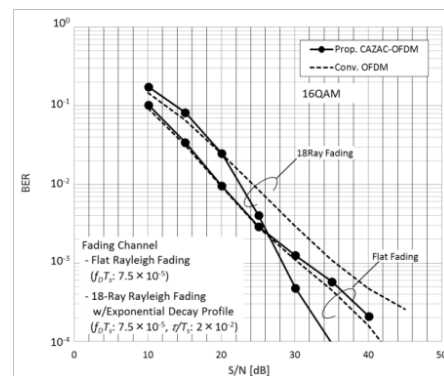


Figure 14. BER performances of the systems under fading channels.